Qualitative Investigation of Transom Stern Flow Ventilation

K. J. Maki (kjmaki@umich.edu), A. W. Troesch (troesch@umich.edu) , and R. F. Beck (rbeck@umich.edu)
University of Michigan, USA

1. Introduction

The transom stern is a popular design choice found in all types of marine vessels. The truncated shape is very popular with naval combatants, is found on high speed commercial ferries, and is wide spread in the recreational market for planing boats. Several advantages of this design feature include weight savings, manufacturing efficiency, and possible resistance reduction in the speed range of vessel operation.

The presence of the transom stern while providing operational benefits, introduces new challenges for the designer to predict performance characteristics. The stream wise discontinuity in the hull geometry either creates a viscous "dead-water region", or with sufficient speed, allows for clean separation of the flow.

Present numerical methods can provide useful results when a judgment of the condition of the flow behind the transom is made before the calculation begins. The purpose of this work is to begin a study into the nature of transom ventilation including its inception.

2. Background

Early research on transom sterns was conducted by Saunders [1957]. He provided advice that the speed of ventilation occurs at a F_T~ 4.0-5.0 (where F_T is the Froude number based on transom draft). More recent observations on naval combatants put the ventilation in the range of F_T ~ 3-3.5.

Analytic and numerical work logically began with a study of a 2-d, local flow model. This model can be described as steady flow past a semi-infinite body of constant draft. Vanden-Broeck and Tuck [1977] describe a potential flow solution with a series expansion in F_T that is valid for low speeds where the transom stagnation point travels vertically upward on the transom as the F_T increases. Vanden-Broeck [1980] offers a second solution applicable to the post ventilation speeds. Physically the low speed solution (A) is valid for low speeds that are typically never seen in experiments due to the viscous separation forming the dead water region.

The same 2-d local case has been studied by Scorpio and Beck [1997]. They use a fully non-linear desingularized potential flow code (DELTA) to investigate this problem. The free surface results of both the low speed (A) and high speed (B) solutions for both the work by Vanden-Broeck [1980] and Scorpio and Beck [1997] are shown in Figure 1. The body is visible on the left of the figure with the flow going from left to right.

The agreement is satisfactory between the two methods, but the question remains as to the behavior of the flow in the speed range between the low speed and ventilation regimes. A useful plot to describe the two solutions is found in Figure 2. Here the non-dimensional wave steepness (peak to trough distance normalized by wavelength) is plotted as a function of F_T. It is interesting to note that the two solutions cross at approximately F_T~2.6. It can be hypothesized that ventilation is physically realized at the crossing point of the two solutions. The fact that the potential flow model suggests ventilation at a F_T that agrees with experimental observations is surprising when the flow exhibits definite viscous effects that are neglected in the potential flow formulation.

For the 3-d full-ship problem, Subranami [2000] extended the fully nonlinear desingularized DELTA code to analyze a body with a transom stern. Additionally, Doctors [2003] among others has strived to suitably model the transom hollow for use in linearized potential flow programs. Doctors has also performed experiments to document the geometry of the hollow. One interesting result from the series of model tests is the F_T of ventilation having a value of approximately 2.5. This agrees closely with Vanden-Broeck and Scorpio hypothesis, but is only half the recommended value of Saunders and less than seen in naval observations.

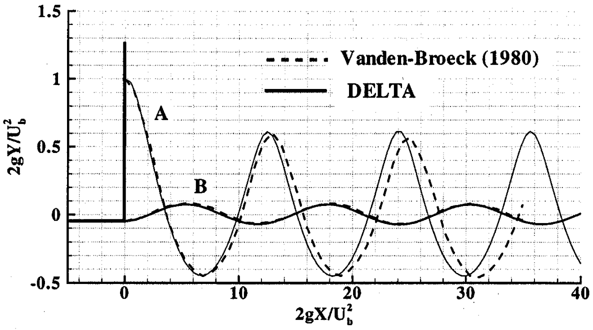

Figure 1. Free surface elevation for both the low speed (A) and high speed (B) solution at F_T = 6.3. Scorpio and Beck [1997]

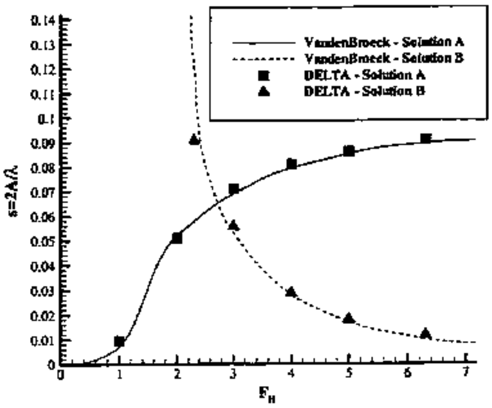

Figure 2. Non-dimensional wave steepness for both the low speed (A) and high speed (B) solution as a function of F_T. Scorpio and Beck [1997]

3. Experimental Results

To document the flow characteristics of transom stern flow near the speeds of ventilation, a set of model tests were performed in the main model basin of the Marine Hydrodynamics Laboratory of the University of Michigan. The models consisted of a block type model, with 0° deadrise, as well as a prismatic model with 20° deadrise. Table 1 summarizes the geometric particulars of the two models. The models were fixed at the bow and the transom draft changed by altering trim, which was kept fixed during a run. The *Re* based on length for both models ~ 2 x 10^6. Runs were conducted for four different drafts for the block, and the prismatic model was tested at one draft.

Possibly the most important parameter of interest to the designer is the speed at which the transom is completely dry, or ventilated. Historically this speed has been documented visually, as in Saunders [1957]. Recently, Doctors [2003] has used a wave probe to measure the free-surface elevation behind the transom of the vessel. The distance the free surface drops below the mean still water plane can conveniently be normalized by the transom draft as suggested by Doctors [2003]:

$$\eta_{dry} = \frac{-\varsigma_{holl}}{T_{tran}} \qquad (1)$$

where ς_{holl} is the vertical distance from the calm waterline to the free surface (positive upwards) and T_{tran} is the vertical distance from the bottom of the transom to the calm waterline on centerline. This new parameter η_{dry} is initially equal to zero (at zero speed) and approaches unity as the vessel attains speed sufficient for ventilation. The primary result of the Marine Hydrodynamics Laboratory experiments is to catalog the ventilation versus speed behavior. Table 2 is a summary of different η_{dry} values at different speeds for both model geometries. The photographs in Plate 1 correspond to the entries in Table 2 for the 7.6 cm draft. Table 3 shows the speed of full ventilation for different drafts of the block model.

Geometry	L (m)	B (m)	T (cm)	B/T	trim (°)
Block	2.17	0.32	2.5	12.8	0.7
Block	2.17	0.32	5.1	6.3	1.3
Block	2.17	0.32	7.6	4.2	2.0
Block	2.17	0.32	10.2	3.1	2.7
Prism	2.09	0.32	7.6	4.2	2.1

Table 1. Model Dimensions.

Geometry	T (cm)	F_T	η_{dry}
Block	7.6	1.45	0.33
Block	7.6	1.74	0.67
Block	7.6	1.97	1
Prism	7.6	1.67	0.42
Prism	7.6	1.78	0.67
Prism	7.6	1.81	1

Table 2. Summary of transom ventilation parameter η_{dry} for different model geometries at different speeds but same draft.

Geometry	T (cm)	F_T	trim (°)	B/T
Block	2.5	2.04	0.7	12.8
Block	5.1	2.01	1.3	6.3
Block	7.6	1.97	2.0	4.2
Block	10.2	1.95	2.7	3.1

Table 3. Summary of transom ventilation speed F_T for the block model at different drafts.

Plate 1 at the end of this abstract contains photographs that represent different stages of ventilation for both the block and prismatic models. The photographs on the left depict the block model and are arranged in increasing speed from top to bottom. The first picture shows the mean free surface in the hollow depressed about one third the still water draft, corresponding to $\eta_{dry} \sim 0.33$. The second picture shows $\eta_{dry} \sim 0.67$, with the third picture at a speed right at ventilation ($\eta_{dry} = 1.0$). The fourth picture is taken well after ventilation, and vertically down to illustrate the wide detached spray region and Kelvin wake.

The pictures on the right are arranged similarly for the prismatic model with increasing speed from top to bottom. The first picture shows a partially ventilated state with $\eta_{dry} \sim 0.4$. The second shows the prismatic model with $\eta_{dry} \sim 0.67$, and the final picture clearly shows full ventilation. It is interesting to note that the bubbly wake has been completely shed very shortly after $\eta_{dry} \rightarrow 1$, while with the block model the bubbly wake is trapped by the wide spread first wave crest. The first wave crest for the prism rises up along the vessel longitudinal centerline but slopes downward transversely, disallowing any bubble entrapment.

As noted in the table and seen in the photographs, the ventilation speed is very near $F_T = 2.0$. This is less than half the speed Saunders [1957] suggests and slightly less than the 2.5-2.6 range hypothesized by Vanden-Broeck [1980] and Scorpio and Beck [1997], and the 2.5 predicted from experiments by Doctors [2003]. The speed for complete ventilation is nearly the same for both cases, with the gradient $\partial\eta_{dry}/\partial F_T$ prior to ventilation being greater for the prismatic model.

The geometrical characteristics of the complex flow (both pre and post ventilation) depend on the shape of the model. The block has a wide or transversely smeared first wave crest, where as the prismatic model has the more common narrow "rooster-tail". The bottom photograph on the left of Plate 1 shows the width of the crest that is about 1/3 the beam for the block model.

As can be seen by observing the flow in the transom region of a ship or model, there is unsteadiness present. In reference to ventilation, the unsteadiness is visible at very low speeds, shortly after the viscous separation from the bottom of the transom and establishment of a separation streamline. At speeds slightly less than $F_{T,ventilation}$, air bubbles begin to form. The bubble formation at the ventilation speed is different for the two different models. The block model kept the bubbles present on the face of the first wave crest whereas the prismatic model's bubbles where convected away from the transom immediately after ventilation.

A transient behavior in the free surface elevation was observed with a period on the order of 3-7 seconds. These transients were more sensitive than expected as speed changes as small as $\pm \Delta F_T \sim 0.10$ were significant enough to create physically visible transients. Due to these observations and the desire to study η_{dry} in approximate steadiness, all photos where taken toward the end of a full-length run of the tank after the transients had dissipated.

The ventilation process of a transom stern has long been known to be a function of many variables, such as F_T, B/T, buttock/trim angle, and deadrise angle. The experiments have shown the importance of trim and B/T; future work will clarify in detail the dependence of transom ventilation on these and other important parameters. The near term objectives of this work are to identify the importance of each parameter while at the same time providing data for numerical code validation. The ultimate goal is to arrive at a regression equation that can be used by designers to define the ventilation speed as a function of the important parameters.

4. Acknowledgement

This research is partially supported by an ONR grant entitled "Design Optimization and Methodology for Stern Flaps", N00014-01-2-0008.

5. References

Doctors, L.J. *Hydrodynamics of the Flow Behind a Transom Stern,* Proceedings of the 29th Israel Conference on Mechanical Engineering, Haifa, Israel, 2003.

Saunders, K.E. *Hydrodynamics in Ship Design*, SNAME, Vol. 2, 1957.

Scorpio, S.M., Beck, R.F. *Two-Dimensional Inviscid Transom Stern Flow*, 12th International Workshop on Water Waves and Floating Bodies, France, 1997.

Subramani, A.K. Computations of highly nonlinear free-surface flows, with applications to arbitrary and complex hull form, PhD Thesis, University of Michigan, 2000.

Vanden-Broeck, J.M. *Nonlinear Stern Waves.* Journal of Fluid Mechanics, Vol. 96, Part 3, 1980.

Vanden-Broeck, J.M., Tuck, E.O. *Computation of Near-Bow or Stern Flows, using Series Expansion in Froude Number.* Proceedings of the 2nd International Conference in Numerical Ship Hydrodynamics, Berkeley, 1977.

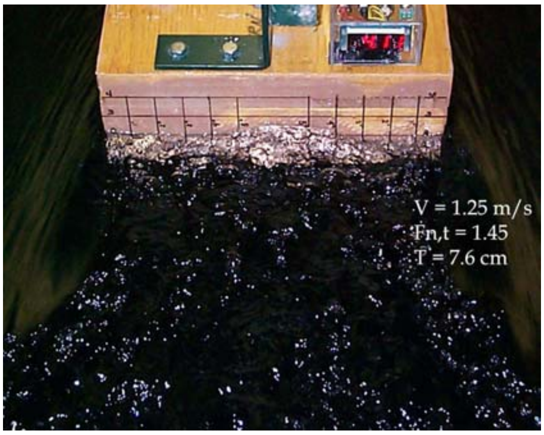

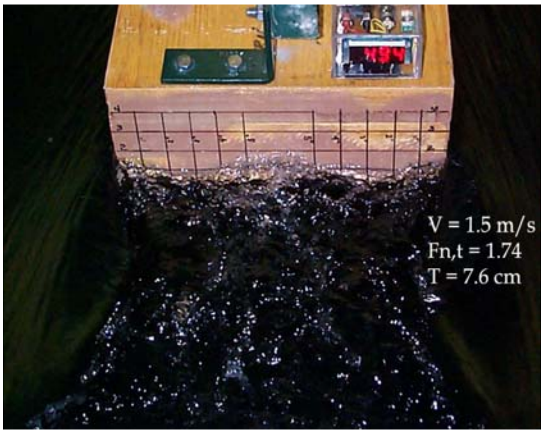

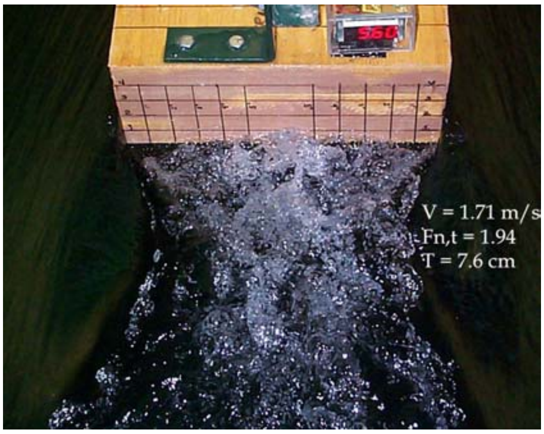

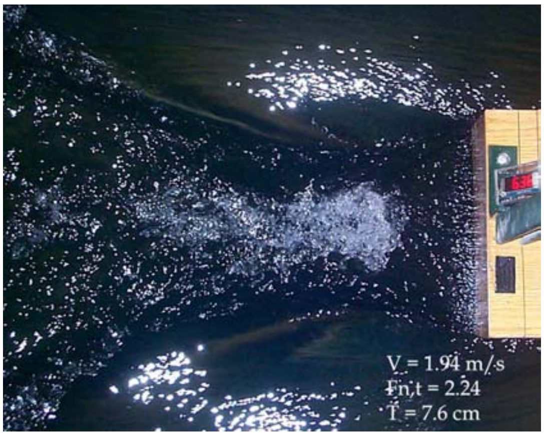

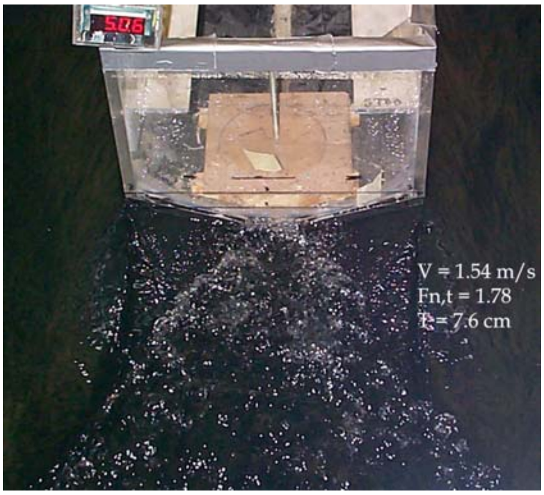

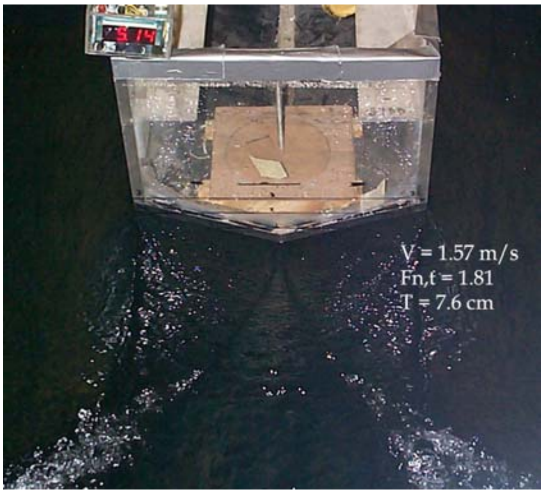

Plate 1. On the left is a sequence of photographs in increasing speed at the same draft from top to bottom. The first two are partially ventilated. The third is just at the onset of full ventilation. The fourth also fully ventilated. On the right is a sequence of the prismatic model. The first two show partial ventilation, while the third is at a speed very near ventilation, but clearly after. Digital display in each photo is speed in feet per second.